CrossMark

ORIGINAL PAPER

Geochemistry of rare earth elements in carbonate rocks of the Mirga Mir Formation (Lower Triassic), Kurdistan Region, Iraq

Faraj H. Tobia[1] · Ahmid M. Aqrawi[1]

Abstract Major trace and rare earth element (REE) concentrations in carbonate rocks of Mirga Mir Formation were analyzed to study the influence of terrigenous materials on REE distribution and to examine REE geochemistry for redox conditions. Contents of SiO_2, Al_2O_3, Fe_2O_3, K_2O, Na_2O, and most of the trace elements are lower than that of a shale standard, whereas the contents of CaO, Nb, and Sr are higher. The REE content however is slightly lower than that in marine carbonate rocks. These values indicate that the carbonates of Mirga Mir Formation possess (1) non-seawater-like REE-Y patterns, (2) positive Gd anomalies (average=1.18), Gd/Gd* ratio of modern shallow seawater, (3) super chondritic Y/Ho ratio is 30.06, and (4) both negative and positive Ce anomalies (Ce/Ce*=0.93–1.12) and most of the samples have slightly positive La anomalies. The carbonate rocks show low U content, authigenic U, and negative Ce anomalies suggesting the deposition under oxic conditions, while the positive anomalies are due to the influence of detrital clays. The present study concludes that the character of the carbonate rocks is masked by the terrigenous sediments.

✉ Faraj H. Tobia
farajabba58@gmail.com

[1] Department of Geology, Salahaddin University, Erbil, Kurdistan Region, Iraq

Introduction

The rare earth elements (REEs; from La through to Lu) are a coherent geochemical group characterized by single oxidation state: REE^{3+} except Ce and Eu. During the last few decades, REEs have become important geochemical tracers in order to understand the chemical evolution of the earth's continental crust (McLennan 1989; Dupré et al. 1996). Many studies indicate that REEs may be mobilized during weathering and that REEs may behave non-conservatively (Sholkovitz et al. 1994).

The distribution of the REEs in marine waters, sediments, and carbonate rocks has been studied by many researchers (De Baar et al. 1988; Elderfield et al. 1990; Madhavaraju and Ramasamy 1999; Armstrong-Altrin et al. 2003; Webb and Kamber 2000; Nothdurft et al. 2004; Madhavaraju and Lee 2009; Madhavaraju et al. 2010; Nagarajan et al. 2011; Madhavaraju and González-León 2012). The concentrations of REEs in seawater are principally influenced by different input sources (e.g., terrestrial input from continental weathering and hydrothermal activities) and scavenging processes related to depth, salinity, and oxygen levels especially Ce (Elderfield 1988; Madhavaraju and González-León 2012).

The REE patterns in carbonate rocks are mainly influenced by depositional environment such as proximity to source area (Murray et al. 1990, 1992; Madhavaraju and Ramasamy 1999), widespread oceanic redox conditions (Liu et al. 1988; German and Elderfield 1990; Murray et al. 1991), diagenetic processes (Scherer and Seitz 1980; Schieber 1988; Armstrong-Altrin et al. 2003; Morad et al. 2010; Fu et al. 2010), variations in surface productivity (Toyoda et al. 1990), lithology (Nath et al. 1992; Madhavaraju and Ramasamy 1999; Armstrong-Altrin et al. 2003; Madhavaraju and Lee 2009; Madhavaraju et al. 2010; Fu

🖄 Springer

et al. 2010), and paleogeography and depositional models (e.g., Kamber and Webb 2001; Kemp and Trueman 2003). REE + Y in carbonates can be affected by fluid mobilization during diagenesis and metamorphism (Holser 1997). Therefore, ancient sedimentary rocks are considered as reliable proxies for REE sources.

The seawater signatures of the carbonates are masked by the incorporation of terrigenous material, which has relatively high non-seawater-like REE contents (Nothdurft et al. 2004; Madhavaraju and Lee 2009; Madhavaraju et al. 2010). The identification of terrigenous particles present in the marine rocks as contaminants is an important aspect of understanding the geochemistry of carbonate rocks.

The aim of this work is to study the REE characteristics in the carbonate rocks of Mirga Mir Formation to determine the influence of terrigenous materials on REE distribution and to examine REE geochemistry for redox conditions.

Geological setting

The Iraqi Northern Thrust Zone is located along the Turkey–Iraq border (Fig. 1). It is ~15 km wide, E-W trending narrow belt between the Hazil Su valley in the west and the Dirri area in the east. It contains Paleozoic and Mesozoic strata which were thrust over the Palaeogene and Neogene clastics and carbonates of the High Folded Zone. The Lower Paleozoic clastic rocks form the soft cores of the two major domes

(Ora to the east and Kaista to the west) flanked by Upper Palaeozoic and Triassic carbonates (Jassim and Goff 2006).

The Triassic and Jurassic sediments are shallow-water carbonates with a thickness of ~2500 m. The Cretaceous succession consists of a thin section of shallow-water carbonates followed by ~500-m-thick siliciclastic sediments. These observations indicate that the southern Neo-Tethys progressively widened during Early Triassic time, and the Cretaceous ridge at the northern margin of the Arabian Shelf was activated during Cretaceous time (Buday and Jassim 1987). A break-up unconformity was formed on the northern and eastern margins of Arabian Plate (Jassim and Goff 2006).

The Lower Triassic rocks that include the Mirga Mir Formation of northern Iraq represent the Neo-Tethys passive margin sediments. These were deposited during an important period of the evolution of the eastern margin of the Afro-Arabian Craton, representing the exposed record of Induan Stage (Sharland et al. 2001). The Mirga Mir Formation is the top impermeable strata overlying Chia Zairi reservoir in some Iraqi oil fields (Edgell 1977; Aqrawi et al. 2010; Balaky 2012).

The Mirga Mir Formation was first described by Wetzel (1950) in the Ora region of Northern Thrust Zone. It comprises 200 m of thinly bedded gray and yellow argillaceous limestone and shale with some recrystallized breccias (Fig. 2); oolitic limestones with rare sandy beds occur near the base of the formation (Bellen et al. 1959). In well Atshan-1 of the Foothill Zone, the formation contains a higher proportion of clastics, probably derived from the Rutba Uplift to the

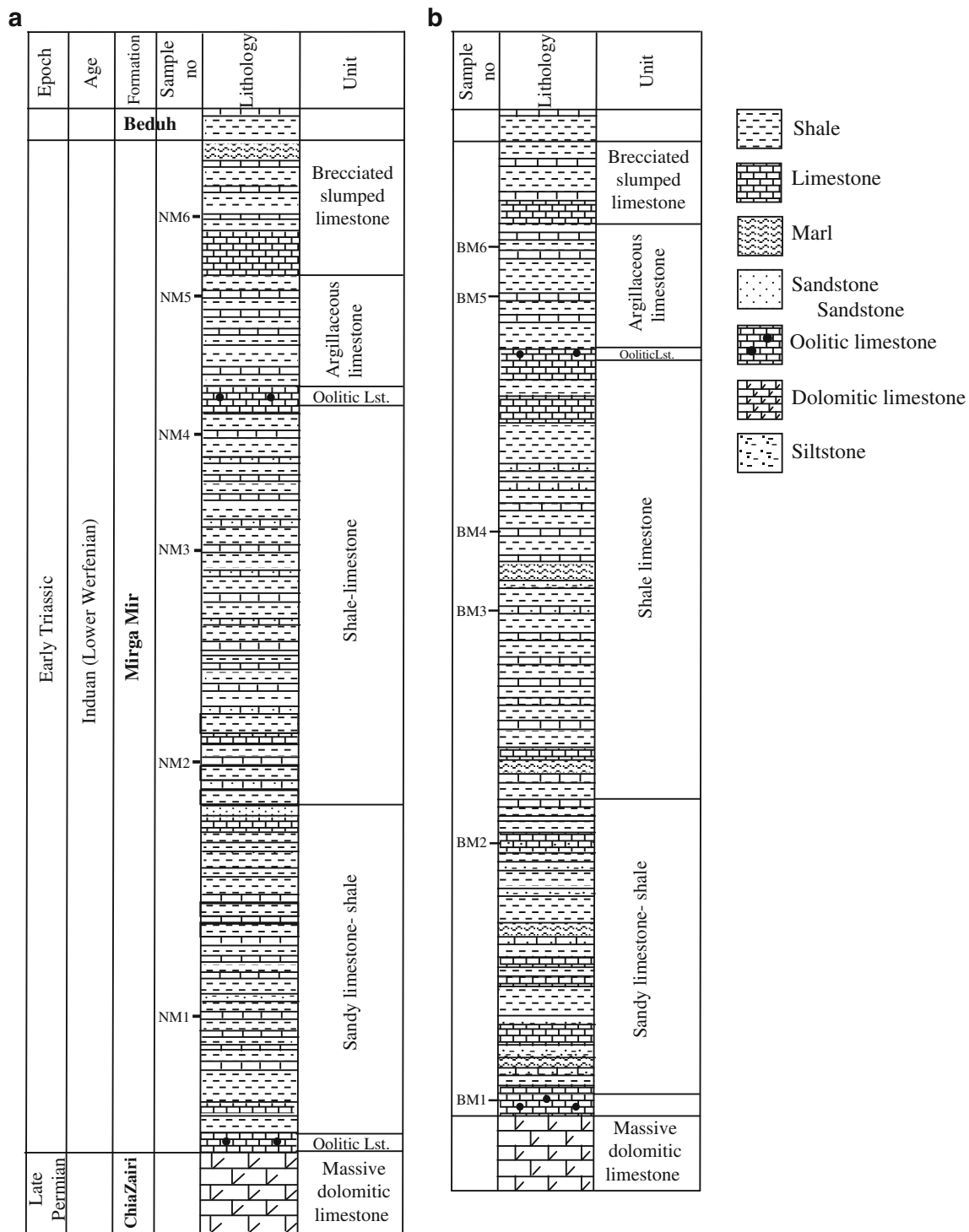Fig. 1 Location and geological map of the northern part of Iraq
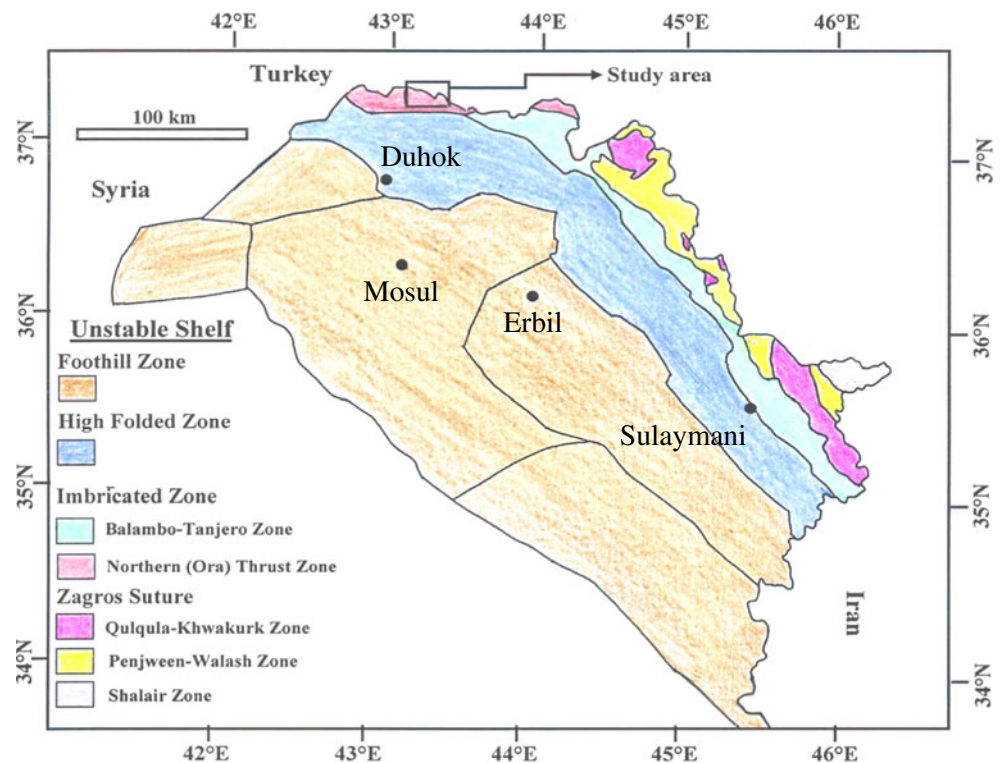
Fig. 2 Stratigraphic columnar sections and location of the studied samples of the Mirga Mir Formation, Northern Thrust Zone. **a** Nazdur section. **b** Beduhe section (modified from Balaky 2012)

southwest. This formation is always underlain by the Chia Zairi Formation and overlain by the Beduh Formation; the contact relationships between them are conformable (Hamza and Issac 1971). It is also crops out in the High Folded Zone of Sirwan gorge in NE Iraq (Bellen et al. 1959; Jassim et al. 2006). On the western Stable Shelf, the most probable

occurrence of this formation is along the western boundary of the Salman Zone. The fossils in the typical section demonstrate that the age of the Mirga Mir Formation is Early Triassic (Werfenian) (Bellen et al. 1959).

According to the results of petrographic, facies, and textural analyses, Balaky (2012) concluded that the Mirga

Mir Formation in Northern Thrust Zone was deposited at a gently sloping epeiric carbonate ramp with two shoreline-detached high-energy belts. The gradual shallowing of the basin is indicated by the offshoal/basinal sediments at the lower part of the formation to backshoal/lagoonal environments with evaporites in the uppermost part of the formation.

In terms of the timing of deposition, the Mirga Mir formation is similar to parts of the Goyan Formation in SE Turkey (Altinli 1966), the upper part of the Dubayyat Group (Dubertret 1966) and the lower part of the Khaneh Kat Formation in SW Iran (Frust 1970), and the Sudair Shale Formation in Saudi Arabia (Powers et al. 1966).

Materials and methods

Twelve carbonate samples of the Mirga Mir Formation were collected from two sections (Figs. 1 and 2) and analyzed in this study. Care was taken to remove the weathered materials from the surface of the samples. Then, the selected samples were air dried and powdered in an agate mortar. Major element composition was obtained by X-ray fluorescence in fused $LiBO_2/Li_2Bi_4O_7$ disks using X-ray fluorescence spectrometer at Acme Laboratories, Vancouver, Canada. Total carbon and sulfur concentration were determined by Leco analysis. The geochemical standards OREAS72B and SY-4(D) were used for quality control. The analytical accuracy errors were better than ±2 % for SiO_2 (0.5 %), Al_2O_3 (0.1 %), Fe_2O_3 (1.1 %), CaO (0.1 %), MgO (1.9 %), Na_2O (0.0 %), and MnO (1.8 %) and better than ±6 % for K_2O and Cr_2O_3 (5.1 and 4.9 %, respectively). The geochemical standard GS311-1 was used for total carbon and sulfur, and the accuracy errors were better than ±1 % for total sulfur (0.4 %) and better than ±5 % for total carbon (4.1 %), respectively.

Trace and rare earth elements were determined by inductively coupled plasma-mass spectrometer. The acid leaching procedure for rare earth elements followed a lithium borate fusion and dilute acid digestion. The geochemical standard SO-18 was used for the calibration of trace and rare earth elements with exception of Cu, Pb, Zn, and Ni where GS311-1 was used. The results were compared with the recommended values. The precision was better than ±2 % for Ba, Cs, U, and Zn (1.8, 1.4, 0.6, and 0.05, respectively) and better than ±6 % for Ga, Th, V, Zr, Y, Mo, Cu, and Pb (5.4, 2.1, 3.8, 2.2, 2.6, 2.7, 5.9, and 4.1 %, respectively). The precision was better than ±4 % for rare earth elements La, Ce, Gd, Dy, Er, Yb, and Lu (3.9, 0.0, 2.4, 3.4, 4, 2.3, and 3.8 %, respectively); ±10 % for Pr and Tm (8.2 and 6.9 %, respectively); and ±15 % for Nd, Sm, Gd, Tb, and Ho (10.2, 14.9, 11.3, 12.8, and 12.7, respectively).

Yttrium is inserted between Dy and Ho in the REE pattern based on its identical charge and similar radius (Bau 1996).

REEs were normalized to the Post-Archean Australian Shale (PAAS) values of Taylor and McLennan (1985).

Results

The major oxide analysis of the carbonate samples from the Mirga Mir Formation is given in Table 1. The content of SiO_2 (4.63–51.42 %, average=16.57 %), Al_2O_3 (0.32–17.67 %, average=4.89 %), Fe_2O_3 (0.41–8.06 %, average=2.10 %), and CaO (3.71–53.97 %, average=40.65 %) between the analyzed samples is variable. Except for CaO, sample NM6 has the highest contents of the major oxides (Table 1), which is similar to that of PAAS. In comparison to PAAS, the Mirga Mir carbonate rocks have lower concentrations of Ba, Co, Cs, Ga, Hf, Rb, Th, U, V, Zr, Y, Cu, Pb, and Zn and higher concentrations of Nb and Sr. In addition, a significant variation is also observed in most of the trace elements (Table 2).

The concentrations of REE are generally lower in carbonate rocks than shales (Table 3). The sediments of high REE concentration show non-seawater-like pattern (Nothdurft et al. 2004; Nagarajan et al. 2011).

PAAS-normalized REE-Y patterns of carbonate rocks of the Mirga Mir Formation are shown in Fig. 3. They exhibit (1) non-seawater-like REE-Y patterns, (2) positive Gd anomalies (average=1.18); Gd/Gd* ratio of modern shallow seawater is 1.05 to 1.30 as suggested by De Baar et al. (1985) and Zhang and Nozaki (1998), (3) super chondritic Y/Ho ratio is 30.06 more or less comparable with the limestone of Mural Formation (34.5±5) (Madhavaraju et al. 2010) and less than the value of seawater (~44–74) as stated by Bau (1996), and (4) Ce/Ce* values (0.93–1.12) are nearly close to 1 as shown in Table 4 and Fig. 4. This reflects the limited Ce anomalies.

With the exception of sample NM6 (187.04 ppm), the ΣREE contents vary from 20.22 to 105.15 which is lower than PAAS (Table 3). The differences of REE content between the analyzed samples result mainly from the amount of the terrigenous materials in the carbonate rocks (Table 1) which effectively mask the seawater characters.

Discussion

Depositional environment

The Ce anomalies in marine carbonate rocks have been considered indicators of contemporaneous paleo-redox conditions (Liu et al. 1988). The deficiency of Ce relative to neighboring rare earth elements can be explained by oxidation of trivalent Ce to less soluble tetravalent Ce and successive removal by suspended particles through the scavenging process (Sholkovitz et al. 1994). However, Ce is remobilized and released into the water column in the suboxic environment

Table 1   Major oxide concentrations (wt%) of the carbonate rocks of the Mirga Mir Formation, Kurdistan Region

Sample no.	Clastic %	Carbonate %	SiO_2	Al_2O_3	Fe_2O_3	CaO	MgO	K_2O	Na_2O	MnO	TiO_2	P_2O_5	L.O.I.	Total
BM1	25.0	75.0	11.33	3.37	1.26	46.07	0.89	0.53	0.27	0.02	0.16	0.02	36.58	100.5
BM2	42.3	57.7	20.85	7.03	2.45	35.89	1.61	1.29	0.27	0.03	0.32	0.03	30.24	100.0
BM3	07.4	92.6	4.63	0.32	0.44	53.97	0.37	0.02	0.10	0.02	0.01	0.02	1.40	101.3
BM4	46.4	53.6	25.80	8.18	2.85	31.99	1.30	1.76	0.55	0.06	0.34	0.06	27.28	100.2
BM5	11.5	88.5	4.65	0.38	0.41	51.74	1.89	0.01	0.13	0.03	0.01	0.02	41.48	100.8
BM6	41.1	58.9	21.56	6.79	2.58	35.24	1.84	1.27	0.30	0.03	0.32	0.05	30.26	100.2
NM1	28.4	71.6	16.03	3.40	1.42	42.79	0.72	0.70	0.17	0.03	0.30	0.03	34.65	100.3
NM2	24.2	75.8	11.75	3.87	1.61	44.49	1.25	0.50	0.17	0.03	0.21	0.04	36.40	100.3
NM3	15.2	84.8	5.09	1.05	0.77	51.83	1.01	0.09	0.10	0.02	0.05	0.01	40.76	100.8
NM4	39.5	60.5	17.73	5.85	2.27	38.99	1.45	0.89	0.25	0.03	0.27	0.04	32.59	100.4
NM5	14.2	85.8	7.96	0.82	1.03	51.04	0.41	0.08	0.17	0.02	0.06	0.02	39.55	101.2
NM6	91.9	08.1	51.42	17.67	8.06	3.71	3.28	5.59	0.24	0.03	0.59	0.17	8.82	99.58
Average	32.3	67.7	16.57	4.89	2.10	40.65	1.34	1.06	0.23	0.03	0.22	0.04	30.00	100.47
PAAS	–	–	62.40	18.78	7.18	1.29	2.19	3.60	1.10	0.11	0.99	0.16	6.00	103.97

BM Beduhe section, *NM* Nazdur section

resulting in a less negative to positive anomaly in seawater (De Baar et al. 1991). La and Ce anomalies were calculated using the Ce/Ce* and Pr/Pr* ratios following the technique of Bau and Dulski (1996) (modified by Webb and Kamber 2000). The studied samples have limited positive and others have negative La and Ce anomalies (Figs. 3 and 4). Ce/Ce* ratio is a function of the relative proportion of a pure water precipitate and clastic contamination, and with increasing clastic contamination, the ratio approaches 1.

Positive Ce anomalies mainly occur due to detrital input (Nath et al. 1997; Madhavaraju and Ramasamy 1999; Madhavaraju and Lee 2009; Madhavaraju et al. 2010), diagenesis (Armstrong-Altrin et al. 2003), scavenging process

(Masuzawa and Koyama 1989), and paleo-redox conditions (Liu et al. 1988).

In this study, the Ce/Ce* values have negative correlation with scavenging-type particle reactive elements (e.g., Ce/Ce* vs Fe, $r = -0.569$) as shown in Table 5. The observed variations in Ce anomalies whether influenced by scavenging process or paleo-redox changes can be tested by other redox-sensitive elements (uranium and authigenic uranium contents).

The post-depositional early diagenesis (especially in the clay minerals) played a significant role in remobilization as well as fractionation of REEs between sediment and seawater. The fractionation of heavy rare earth elements (HREEs)

Table 2   Trace element concentrations (ppm) of the carbonate rocks of the Mirga Mir Formation

Sample no.	Ba	Co	Cs	Ga	Hf	Nb	Rb	Sr	Th	U	V	Zr	Y	Cu	Pb	Zn
BM1	41	3.0	1.2	4.7	0.8	4.1	23.5	1301	2.8	1.8	24	36.4	7.0	2.8	1.8	14
BM2	83	7.0	2.5	9.7	1.7	7.9	53.9	800	4.7	1.8	44	68.3	9.7	5.1	5.2	23
BM3	16	1.1	0.1	0.5	0.2	0.3	1.1	303	0.4	0.9	8	7.3	3.3	3.7	8.2	6
BM4	285	8.2	3.2	10.8	2.0	6.8	66.5	846	6.9	2.5	53	80.1	16.0	22.1	5.5	38
BM5	14	1.2	0.1	0.5	0.2	0.4	1.0	299	0.7	0.3	8	19.0	6.6	1.4	3.1	87
BM6	83	7.2	2.5	9.3	1.9	8.5	52.1	449	5.1	1.5	44	77.4	11.3	5.7	4.6	25
NM1	33	5.3	1.2	4.5	1.7	6.3	21.2	526	4.5	1.0	24	77.1	13.0	4.4	4.9	8
NM2	57	4.6	1.6	5.5	1.1	5.3	27.6	1187	3.5	1.1	30	45.6	8.3	4.2	4.2	16
NM3	13	1.9	0.2	1.6	0.3	1.3	5.7	576	1.0	0.6	12	13.8	4.8	1.1	1.4	4
NM4	73	4.2	2.2	8.6	1.9	7.7	44.0	832	4.8	1.3	42	68.2	10.3	9.4	2.0	24
NM5	114	1.8	0.1	0.9	0.8	1.3	3.9	653	1.0	0.5	9	25.6	4.4	0.8	2.0	4
NM6	299	9.7	11.1	24.9	4.3	13.2	180.0	38	16.2	2.8	105	131.5	26.0	23.1	7.2	58
Average	92.58	4.60	2.17	6.79	1.41	5.26	40.04	650.8	4.30	1.34	33.58	54.19	10.06	6.98	4.18	25.58
PAAS	650	23	15		5	19	160	200	14.6	3.1	150	210	27	50	20	85

Table 3   Rare earth element concentrations (ppm) of the carbonate rocks of the Mirga Mir Formation

Sample no.	La	Ce	Pr	Nd	Sm	Eu	Gd	Tb	Dy	Ho	Er	Tm	Yb	Lu	LREE	HREE	REE
BM1	10.3	19.9	2.37	9.9	1.76	0.34	1.56	0.23	1.21	0.22	0.63	0.09	0.64	0.09	44.57	4.67	49.24
BM2	18.4	34.1	3.88	13.8	2.50	0.49	2.28	0.33	1.72	0.36	1.06	0.14	0.93	0.14	73.17	6.96	80.13
BM3	4.1	9.0	0.98	3.3	0.66	0.17	0.79	0.10	0.47	0.10	0.28	0.04	0.20	0.03	18.21	2.01	20.22
BM4	22.3	43.8	4.93	19.8	3.64	0.74	3.17	0.48	2.41	0.52	1.50	0.23	1.43	0.20	95.21	9.94	105.15
BM5	7.8	20.6	2.37	9.8	1.86	0.42	1.82	0.24	1.24	0.24	0.56	0.06	0.35	0.06	42.85	4.57	47.42
BM6	19.0	35.8	4.05	15.3	2.57	0.54	2.37	0.34	2.27	0.37	1.17	0.17	1.14	0.15	77.26	7.98	85.24
NM1	15.2	32.1	3.65	15.1	3.08	0.63	2.95	0.40	2.32	0.45	1.17	0.17	1.18	0.17	69.76	8.81	78.57
NM2	13.1	26.1	3.00	12.0	2.01	0.43	1.85	0.24	1.56	0.26	0.82	0.13	0.73	0.10	56.64	5.69	62.33
NM3	6.6	16.3	2.13	8.7	1.87	0.37	1.65	0.19	1.12	0.14	0.41	0.05	0.31	0.06	35.97	3.93	39.90
NM4	17.1	33.4	3.74	14.7	2.43	0.46	2.17	0.30	1.78	0.36	1.08	0.15	1.07	0.15	71.83	7.06	78.89
NM5	4.2	9.8	1.33	5.2	1.17	0.23	1.13	0.15	0.86	0.15	0.35	0.06	0.24	0.05	21.93	2.99	24.92
NM6	39.3	76.0	9.30	35.7	6.82	1.32	5.66	0.82	5.08	0.96	2.74	0.42	2.53	0.39	168.44	18.6	187.04
Average	14. 8	29.7	3.48	13.6	2.53	0.51	2.28	0.32	1.84	0.34	0.98	0.14	0.90	0.13	64.65	6.93	71.59
PAAS	38.2	78.6	8.83	33.9	5.55	1.08	4.66	0.77	4.68	0.99	2.85	0.41	2.82	0.43	166.16	17.61	183.77

during early diagenetic recrystallization is primarily controlled by HREE-carbonate complexation in the solution flushing the sediment/pore water system, whereas the light rare earth elements (LREEs) are controlled by reactions involving the continentally derived particulates within the sediments (Mazumdar et al. 2003).

Compared to HREEs, the behavior of the LREEs in Mirga Mir carbonates cannot be explained by carbonate complexation reaction. However, reactions involving LREE-enriched particles in the sediment–water system may impart REEs into carbonates during recrystallization. In addition, the presence of authigenic clay minerals such as mixed layer illite-smectite in several

samples (Balaky 2012) indicates dissolution/reprecipitation of silicate phases. Such reactions mobilize silicate phase-hosted REEs and may affect the LREE abundances during recrystallization of carbonate sediments.

Mode of occurrence of REE

The absorption of fine-grained minerals (e.g., clay minerals) and organic matter may be the main mode of occurrence of REEs. The ΣREE contents of carbonate samples from the Mirga Mir Formation are positively correlated with the Al_2O_3. The significant correlation

Fig. 3 Post-Archean Australian Shale (PAAS) normalized REE patterns for the carbonate rocks of the Mirga Mir Formation
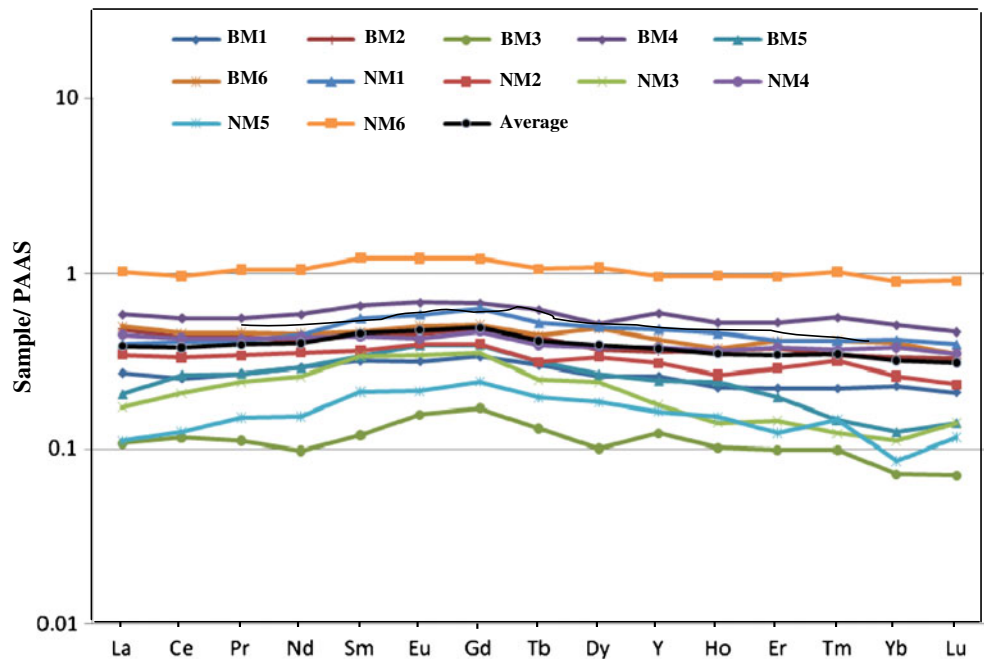
Table 4 Elemental ratios and anomalies of the carbonate rocks of the Mirga Mir Formation

Sample no.	Ce/Ce*	Eu/Eu*	Pr/Pr*	Gd/Gd*	$(La/Yb)_n$	$(Nd/Yb)_n$	$(Dy/Yb)_n$	Er/Nd	Y/Ho	Authigenic U (ppm)	Th/U	Th/Cr	Cr/Th	La/Co	Th/Co
BM1	0.94	0.97	0.98	1.10	1.19	1.29	1.14	0.064	31.82	0.87	1.56	0.82	1.21	3.43	0.93
BM2	0.94	0.97	1.05	1.12	1.46	1.23	1.11	0.077	26.94	0.23	2.61	0.20	5.09	2.63	0.67
BM3	1.05	1.11	1.05	1.34	1.51	1.37	1.42	0.085	33.00	0.77	0.44	0.12	8.50	3.73	0.36
BM4	0.98	1.03	0.98	1.07	1.15	1.15	1.02	0.076	30.77	0.20	2.76	0.29	3.48	2.72	0.84
BM5	1.12	1.07	0.97	1.22	1.65	2.33	2.13	0.057	27.50	0.07	2.33	0.07	14.71	6.50	0.58
BM6	0.95	1.03	1.01	1.13	1.24	1.12	1.20	0.076	30.54		3.40	0.37	2.69	2.64	0.71
NM1	1.01	0.98	0.97	1.19	0.95	1.06	1.18	0.077	28.89		4.50	0.16	6.09	2.87	0.85
NM2	0.97	1.05	0.99	1.21	1.32	1.37	1.29	0.068	31.92		3.18	0.20	4.89	2.85	0.76
NM3	1.02	0.99	1.04	1.28	1.57	2.33	2.18	0.047	34.29	0.27	1.67	0.10	10.3	3.47	0.53
NM4	0.98	0.94	0.99	1.15	1.18	1.14	1.00	0.073	28.61		3.69	0.23	4.27	4.07	1.14
NM5	0.97	0.94	1.08	1.21	1.29	1.80	2.16	0.067	29.33	0.17	2.00	0.15	6.80	2.33	0.56
NM6	0.93	1.00	1.04	1.09	1.15	1.17	1.21	0.077	27.08		5.79	0.34	2.96	4.05	1.67
Average	0.99	1.01	1.01	1.18	1.31	1.45	1.42	0.070	30.06		2.83	0.25	5.92	3.44	0.80

Ce/Ce*= $Ce_n/(La_n*Pr_n)^{0.5}$; Eu/Eu*= $Eu_n/(Sm_n*Gd_n)^{0.5}$, Pr/Pr*= $[Pr/(0.5Ce+0.5Nd)]_n$; Gd/Gd*= $[Gd/(0.33Sm+0.67Tb)]_n$; Authigenic U= total U-(Th/3)

coefficient indicates that the REEs of carbonate samples occur mainly in aluminosilicate minerals which are also supported by significant positive correlations between ΣREE content and SiO_2, K_2O, and MgO (Table 5). In contrast, the ΣREE contents show negative correlation with organic carbon ($r=-0.976$, $n=12$) and organic sulfur ($r=-0.324$, $n=12$).

Illite is the major clay mineral present in all studied samples of the Mirga Mir Formation and kaolinite is the second abundant clay, whereas chlorite is relatively low. Some clay minerals are of detrital origin. A diagenetic origin is also probable through conversion of smectite, kaolinite, and chlorite to illite but the presence of mixed layer clays supports the diagenetic origin (Balaky 2012). Illite is characterized by enrichment of the REE.

Fig. 4 Plot of Ce anomaly (Ce/Ce*) vs the Pr anomaly (Pr/Pr*) for limestone of the Mirga Mir Formation (after Bau and Dulski 1996). The range of modern seawater is shown by the *shaded area* (Nagarajan et al. 2011)

Source of rare earth elements

The enrichment and depletion of REE in limestones may be influenced by various factors: (i) addition of terrigenous particles from the continent (McLennan 1989), (ii) biogenic sedimentation from the overlying seawater (Murphy and Dymond 1984), (iii) scavenging process related to depth, salinity, and oxygen levels (Elderfield 1988; Greaves et al. 1999), and (v) authigenic removal of REE from the water column and early diagenesis (Sholkovitz 1988). Seawater contributes lesser amounts of REE to the chemical sediments, but the samples with non-seawater-like pattern exhibit higher REE concentration (Nothdurft et al. 2004) due to the contamination with non-carbonate materials such as silicates, Fe-Mn oxides, phosphates, or sulfides during the chemical leaching (Zhao et al. 2009; Nagarajan et al. 2011). If carbonate minerals precipitated in equilibrium with seawater, then they typically possess negative Ce anomalies, which may also be reflected in the REE patterns of limestone (Palmer 1985).

Significant variations in ΣREE content of carbonate rocks are noticed in the Mirga Mir Formation from 20 to 187 ppm with an average of 72 ppm (Table 3). This average is more or less comparable with shallow-marine carbonate and Arabian Sea carbonate sediments (73 ± 20 and 78 ± 40 ppm, respectively) (Nath et al. 1997; Madhavaraju and Ramasamy 1999). Differences in ΣREE content among the individual samples are mainly due to variations in the amount of terrigenous sediments included in these limestones. REEs show very strong positive inter-elemental relationships (>0.955, $n=12$) as shown in Table 6, indicating their coherent nature, which also reveals that they are closely related to the terrigenous
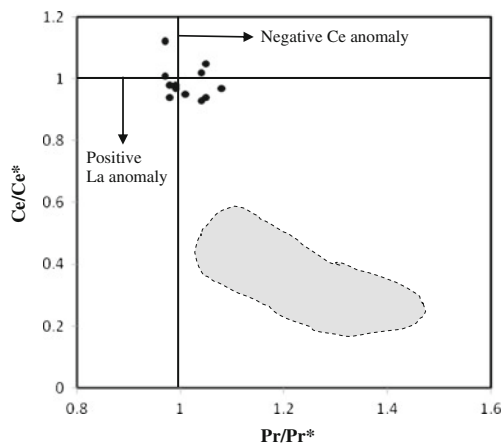
Table 5 Correlation coefficient matrix for major, trace, and total rare earth elements of the carbonate rocks of the Mirga Mir Formation

	SiO₂	Al₂O₃	Fe₂O₃	CaO	MgO	K₂O	Na₂O	MnO	TiO₂	P₂O₅	L.O.I.	REE	Ba	Co	Cs	Ga	Hf	Nb	Rb	Sr	Th	U	V	Zr	Y	Cu	Pb	Zn
SiO₂	1																											
Al₂O₃	0.992	1																										
Fe₂O₃	0.981	0.980	1																									
CaO	-0.997	-0.997	-0.986	1																								
MgO	0.797	0.823	0.829	-0.833	1																							
K₂O	0.978	0.972	0.994	-0.981	0.828	1																						
Na₂O	0.493	0.501	0.364	-0.475	0.233	0.361	1																					
MnO	0.416	0.411	0.292	-0.405	0.270	0.307	0.846	1																				
TiO₂	0.953	0.949	0.896	-0.948	0.710	0.881	0.548	0.467	1																			
P₂O₅	0.948	0.939	0.978	-0.953	0.822	0.981	0.306	0.300	0.836	1																		
L.O.I.	-0.458	-0.448	-0.480	0.441	-0.232	-0.515	-0.048	-0.043	-0.330	-0.537	1																	
REE	0.978	0.974	0.955	-0.983	0.849	0.957	0.476	0.476	0.948	0.933	-0.372	1																
Ba	0.841	0.823	0.813	-0.825	0.564	0.816	0.698	0.651	0.740	0.809	-0.381	0.796	1															
Co	0.902	0.903	0.821	-0.896	0.667	0.811	0.681	0.615	0.960	0.757	-0.298	0.897	0.771	1														
Cs	0.972	0.972	0.995	-0.978	0.840	0.997	0.336	0.283	0.878	0.985	-0.510	0.954	0.796	0.798	1													
Ga	0.989	0.999	0.982	-0.995	0.831	0.973	0.477	0.386	0.944	0.941	-0.452	0.972	0.807	0.890	0.975	1												
Hf	0.984	0.971	0.959	-0.978	0.756	0.943	0.460	0.390	0.970	0.919	-0.401	0.965	0.794	0.897	0.941	0.969	1											
Nb	0.922	0.931	0.871	-0.924	0.726	0.843	0.513	0.397	0.984	0.798	-0.297	0.916	0.661	0.933	0.849	0.931	0.951	1										
Rb	0.987	0.991	0.995	-0.993	0.839	0.993	0.422	0.348	0.910	0.970	-0.490	0.966	0.823	0.849	0.994	0.992	0.957	0.885	1									
Sr	-0.311	-0.252	-0.358	0.306	-0.416	-0.399	0.289	0.081	-0.136	-0.434	0.497	-0.312	-0.193	-0.100	-0.370	-0.255	-0.280	-0.096	-0.328	1								
Th	0.991	0.985	0.985	-0.992	0.806	0.985	0.433	0.387	0.940	0.967	-0.454	0.984	0.819	0.868	0.984	0.984	0.977	0.905	0.988	-0.309	1							
U	0.864	0.883	0.806	-0.857	0.575	0.814	0.741	0.545	0.855	0.749	-0.462	0.824	0.810	0.867	0.805	0.873	0.812	0.820	0.848	0.047	0.841	1						
V	0.988	0.999	0.976	-0.993	0.825	0.966	0.506	0.425	0.947	0.938	-0.448	0.974	0.821	0.900	0.969	0.999	0.969	0.933	0.988	-0.238	0.983	0.881	1					
Zr	0.948	0.932	0.886	-0.941	0.718	0.872	0.544	0.490	0.989	0.837	-0.301	0.951	0.744	0.942	0.866	0.926	0.975	0.970	0.895	-0.203	.934	0.809	0.930	1				
Y	0.966	0.946	0.932	-0.962	0.782	0.941	0.497	0.518	0.937	0.925	-0.381	0.987	0.821	0.884	0.932	0.940	0.957	0.884	0.940	-0.325	0.975	0.814	0.944	0.951	1			
Cu	0.863	0.858	0.823	-0.854	0.618	0.836	0.692	0.710	0.792	0.831	-0.499	0.861	0.930	0.798	0.824	0.849	0.823	0.726	0.850	-0.222	0.861	0.861	0.867	0.794	0.881	1		
Pb	0.472	0.446	0.442	-0.453	0.268	0.488	0.141	0.279	0.413	0.507	-0.872	0.428	0.395	0.456	0.471	0.438	0.416	0.350	0.464	-0.492	0.458	0.452	0.440	0.395	0.455	0.496	1	
Zn	0.357	0.362	0.369	-0.390	0.728	0.406	0.172	0.375	0.229	0.439	-0.034	0.455	0.336	0.234	0.406	0.362	0.289	0.211	0.394	-0.414	0.370	0.199	0.364	0.291	0.436	0.387	0.152	1

More than 0.655 correlation is significant at 0.01 level (2-tailed)

Table 6 Correlation coefficient matrix for the rare earth elements of the carbonate rocks of the Mirga Mir Formation

	La	Ce	Pr	Nd	Sm	Eu	Gd	Tb	Dy	Ho	Er	Tm	Yb	Lu	REE
La	1														
Ce	0.995	1													
Pr	0.990	0.997	1												
Nd	0.983	0.994	0.997	1											
Sm	0.959	0.977	0.987	0.992	1										
Eu	0.955	0.976	0.984	0.989	0.997	1									
Gd	0.957	0.976	0.983	0.988	0.997	0.998	1								
Tb	0.968	0.983	0.986	0.990	0.994	0.994	0.996	1							
Dy	0.966	0.979	0.987	0.989	0.990	0.989	0.990	0.987	1						
Ho	0.973	0.985	0.986	0.987	0.987	0.986	0.990	0.996	0.987	1					
Er	0.991	0.995	0.994	0.992	0.981	0.980	0.982	0.989	0.986	0.994	1				
Tm	0.982	0.984	0.985	0.984	0.975	0.973	0.973	0.982	0.983	0.988	0.995	1			
Yb	0.987	0.986	0.980	0.981	0.966	0.962	0.968	0.978	0.976	0.984	0.994	0.991	1		
Lu	0.982	0.987	0.989	0.989	0.985	0.979	0.984	0.989	0.987	0.994	0.996	0.993	0.993	1	
REE	0.994	0.999	0.998	0.996	0.983	0.980	0.981	0.987	0.984	0.988	0.997	0.988	0.988	0.991	1

More than 0.655 correlation is significant at 0.01 level (2-tailed)

siliciclastic during weathering and REE fractionation (Mazumdar et al. 2003; Nagarajan et al. 2011) and is an evidence of very strong bonds between various REE.

PAAS-normalized REE + Y patterns (Fig. 3) of the Mirga Mir carbonate rocks exhibit flat LREE patterns in some samples and relative HREE depletion in others, in addition to negative Ce anomalies and positive Gd anomalies. The observed $(Nd/Yb)_n$ ratio (average=1.45) of the present samples is more or less similar to that of shallow-marine carbonate (1.51±0.30) (Madhavaraju and Ramasamy 1999) (Table 7).

The $(La/Yb)_n$ ratios range from 0.95 to 1.65 with an average of 1.31 which is similar to the values of terrigenous particulate matter (1.30; Sholkovitz 1990).

The $(Dy/Yb)_n$ ratio of carbonate of the Mirga Mir Formation varies from 1.00 to 2.18 (average=1.42) which is similar to the shallow-marine carbonate (1.25±0.23) (Madhavaraju and Ramasamy 1999) and Indian Ocean carbonate sediments (1.37±0.05) (Nath et al. 1992) (Table 7).

The effects of LREE/HREE fractionation in modern and ancient marine systems can be documented by the Er/Nd ratio (German and Elderfield 1989; Nagarajan et al. 2011). The Er/Nd ratio in normal seawater is about 0.27 (De Baar et al. 1988). The high Er/Nd ratio of limestones effectively reveals the seawater signature retained by the marine carbonate. Addition of detrital material or diagenesis process can reduce the Er/Nd value to <0.1 due to preferential concentration of Nd relative to Er (De Baar et al. 1988; German and Elderfield 1989; Bellanca et al. 1997). The Er/Nd ratios of the carbonate rocks of the Mirga Mir Formation vary between 0.047 and 0.085 with an average of 0.070 (Table 4) and are comparable to shallow-marine carbonate (Madhavaraju and Ramasamy 1999) (Table 7) indicating

the influence of detrital material. The carbonates precipitated from seawater may have variable degrees of contamination (e.g., shale contamination) that would have suppressed the seawater signature, which effectively masks the seawater characteristics.

The influence of terrigenous materials in the carbonate rocks may be assessed by the relative abundance of Al, Zr, Y, Hf, and Th values. Al, Fe, Ti, Th, Rb, and Ce concentrations show significant positive correlations between themselves (Table 5) indicating that Ce is partially related to detrital input along with the original seawater fractionation. Positive correlation of ΣREE with Al_2O_3 ($r=0.974$, $n=12$) and negative correlation with CaO ($r=-0.983$, $n=12$) (Table 5) imply the presence of terrigenous fractions, which may be the possible source of REE in these carbonate rocks. The terrigenous source of REE is further confirmed by the strong positive correlation between ΣREE and Fe_2O_3, Ni, Th, Cr, and Y (Table 5). The significant correlation between the major oxides (Al_2O_3, Fe_2O_3, TiO_2, and MnO) confirms the presence of detrital input to the basin during the deposition. On the other hand, the Ca concentration shows negative relationship with the detrital components (Table 5), which is consistent with Ca precipitated mainly with shallow-water carbonates.

The Th/Cr ratios are widely used to constrain the provenance composition of the source region, based on their discrimination of felsic and mafic rocks (Wronkiewicz and Condie 1990; Cox et al. 1995; Cullers 1995, 2000; Armstrong-Altrin et al. 2004; Armstrong-Altrin 2009). Th/Cr, La/Co, and La/Th ratios of carbonate rocks of the Mirga Mir Formation (Table 4) are compared with felsic and mafic

Table 7 Average values of the carbonate sediments of the Mirga Mir Formation (this study) compared to the values of shallow and deep-water marine carbonate sediments

Element ratio	Mirga Mir carbonate sediments[a]	Shallow marine carbonate[b]	Arabian Sea carbonate sediments[c]	Indian Ocean carbonate sediments[d]	Yellowish limestone[e]
Ce/Ce*	0.99	0.76±0.16	0.84±0.06	0.56	0.57±0.05
$(La/Yb)_n$	1.31	1.82±0.46	0.85±0.2	0.166±0.953	0.71±0.15
Gd/Gd*	1.18		1.09±0.04		0.98±0.20
$(Nd/Yb)_n$	1.45	1.51±0.30	0.85±0.17	0.83±0.13	0.42±0.09
$(Dy/Yb)_n$	1.42	1.25±0.17	1.12±0.11	1.37±0.05	1.19±0.11
Y/Ho	30.06		34.14±1.64		31.11±9.17
Er/Nd	0.07	0.07±0.02	0.11±0.02		0.2±0.02
Eu/Eu*	1.01	0.58±0.11	1.15±0.08	>1	1.88±1.009
REE (ppm)	71.78	73±20	78±40		25.55±9.914

[a] This study

[b] Madhavaraju and Ramasamy (1999)

[c] Nath et al. (1997)

[d] Nath et al. (1992)

[e] Nagarajan et al. (2011)

rocks (fine fraction) as well as to the average upper continental crust (UCC) and PAAS values (Table 8), which suggests a source of felsic rocks.

Redox-sensitive element and REE application for palaeo-environmental analysis

Oxygen levels in water influence the oxidation state of some trace elements and control their solubility in seawater and their enrichment in marine sediments (Arnaboldi and Meyers 2007; Azmy et al. 2009; Hua et al. 2013). From the trace element concentrations of the sediments, we can estimate the oxidation state of the bottom water and sediments during deposition (Hua et al. 2013).

Uranium is mobilized as U^{6+} in oxic environments and precipitates as U^{4+} in reducing environments (Anderson et al. 1983; Wright et al. 1984). Similarly, vanadium is oxidized to soluble V^{6+} under oxic environments and reduced to V^{4+} and forms insoluble $VO(OH)_2$ under mildly reducing conditions (Wanty and Goldhaber 1992). Other redox-sensitive elements such as Co and Cr behave in a similar way, which tends to be more soluble under oxidizing conditions (Algeo and Maynard 2004).

The concentration of authigenic uranium (authigenic U= total U-Th/3) has also been used to understand the redox change in the marine environments (Wignall and Myers 1988). The authigenic uranium content of the analyzed samples is less than 2 ppm (Table 4) which suggests oxic conditions of deposition.

The Ce anomaly in marine carbonate rocks was used as an indicator of palaeo-redox conditions. Many studies have been undertaken on Ce behavior in marine environments to estimate the palaeo-oceanographic conditions (Liu et al. 1988; German and Elderfield 1990; Nath et al. 1997). As marine waters show negative Ce anomaly, similar Ce anomaly in limestone reveals the inclusion of REE directly from seawater or pore water under oxic conditions. The negative Ce anomaly can be explained by oxidation of Ce^{3+} to less soluble Ce^{4+} and successive removal by suspended particles through scavenging process (Sholkovitz et al. 1994; Madhavaraju and

Table 8 Range and elemental ratios of carbonate rocks of the Mirga Mir Formation compared to felsic, mafic rocks, Upper Continental Crust (UCC), and Post-Archean Australian Shale (PAAS)

Ratios	Range of present study	Range of felsic rocks[a]	Range of mafic rocks[a]	UCC[a]	PAAS[b]
Eu/Eu*	0.94–1.11	0.40–0.94	0.71–0.95	0.63	0.66
Th/Cr	0.07–0.82	0.13–2.7	0.018–0.046	0.13	0.13
Cr/Th	1.21–14.71	4.00–15.00	25.00–500	7.76	7.53
La/Co	2.33–6.50	1.80–13.80	0.14–0.38	1.76	1.65
Th/Co	0.36–1.14	0.67–19.40	0.04–1.40	0.63	0.63

[a] Cullers (2000)

[b] Taylor and McLennan (1985)

González-León 2012). However, Ce is remobilized into the water column in the suboxic environment resulting in a less negative to positive anomaly in seawater (De Baar et al. 1991).

The carbonate samples from the Mirga Mir Formation show low values of redox-sensitive elements (e.g., U, V, Co, and Cr) (Table 2). Six samples show slightly negative Ce anomalies and the others show slightly positive Ce anomalies. The former are due to the oxic conditions while the positive are due to the influence of detrital input (Madhavaraju and Ramasamy 1999; Madhavaraju and Lee 2009; Nath et al. 1997), scavenging process (Masuzawa and Koyama 1989), and palaeo-redox conditions (Liu et al. 1988).

Conclusions

The carbonates of the Mirga Mir Formation show limited positive and negative La and Ce anomalies. The variations in Ce anomalies in these limestones were controlled by the detrital input, scavenging process, and diagenesis (especially in the clay minerals). The low contents of U and authigenic U of limestones of the Mirga Mir Formation suggest that these limestones were deposited under oxic conditions. Th/Cr ratios are in the range indicative of the felsic rocks.

The limestones possess moderate ΣREE contents, moderate $(La/Yb)_n$ ratios, and non-seawater-like REE-Y patterns suggesting that the REE concentrations were mainly derived from the terrigenous sediments.

These limestones were affected by effective shale contamination which masked their original seawater pattern. These results indicate that the original seawater-like REE + Y patterns were changed in the limestones due to the contamination with very large amounts of terrigenous materials.

References

Algeo TJ, Maynard J (2004) Trace element behavior and redox facies in core shales of Upper Pennsylvanian Kansas-type cyclothems. Chem Geol 206(3–4):289–318

Altinli IE (1966) Geology of eastern and southeastern Anatolia. Turkey Min. Rep. Explor. Inst. Bull., Foreign Edition, Ankara 60: 35–76

Anderson R, Bacon MP, Brewer PG (1983) Removal of ^{230}Th and ^{234}Pb at ocean margins. Earth Planet Sci Lett 66:73–90

Aqrawi AAM, Goff JC, Horbury AD, Sadooni FN (2010) The petroleum geology of Iraq. Statoil Scientific Press: 424 p

Armstrong-Altrin JS (2009) Provenance of sands from Cazones, Acapulco, and Bahía Kino beaches, Mexico. Revista Mexicana de Ciencias Geológicas 26:764–782

Armstrong-Altrin JS, Verma SP, Madhavaraju J, Lee YI, Ramasamy S (2003) Geochemistry of Late Miocene Kudankulam Limestones, South India. Int Geol Rev 45:16–26

Armstrong-Altrin JS, Lee YI, Verma SP, Ramasamy S (2004) Geochemistry of sandstones from the Upper Miocene Kudankulam Formation, southern India: implications for provenance, weathering, and tectonic setting. J Sediment Res 74:285–297

Arnaboldi M, Meyers PA (2007) Trace element indicators of increased primary production and decreased water column ventilation during deposition of latest Pliocene sapropels at five locations across the Mediterranean Sea. Palaeogeogr Palaeoclimatol Palaeoecol 249(3–4):425–443

Azmy K, Sylvester P, de Oliveira TF (2009) Oceanic redox conditions in the Late Mesoproterozoic recorded in the upper Vazante Group carbonates of Sao Francisco Basin, Brazil, evidence from stable isotopes and REEs. Precambrian Res 168(3–4):259–270

Balaky SM (2012) Sedimentology and stratigraphy of Mirga Mir Formation (Lower Triassic) in the Northern Thrust Zone, Iraqi Kurdistan Region. Unpublished Ph.D. Thesis, Salahaddin University: 176p

Bau M (1996) Controls on the fractionation of isovalent trace elements in magmatic and aqueous systems: evidence from Y/Ho, Zr/Hf, and lanthanide tetrad effect. Contrib Mineral Petrol 123:323–333

Bau M, Dulski P (1996) Anthropogenic origin of positive gadolinium anomalies in river waters. Earth Planet Sci Lett 143:245–255

Bellanca A, Masetti D, Neri R (1997) Rare earth elements in limestone/marlstone couplets from the Albian-Cenomanian Cismon section (Venetian region, northern Italy): assessing REE sensitivity to environmental changes. Chem Geol 141:141–152

Bellen RC, Van Dunnington HV, Wetzel R, Morton DM (1959) Lexique Stratigraphique International. V. III, Asie, Fasc., 10a Iraq. Paris: 333 p

Buday T, Jassim SZ (1987) The regional geology of Iraq: tectonism, magmatism and metamorphism, vol 2. Publications of GEOSURV, Baghdad, p 352

Cox R, Low DR, Cullers RL (1995) The influence of sediment recycling and basement composition on evolution of mudrock chemistry in the southwestern United States. Geochim Cosmochim Acta 59: 2919–2940

Cullers RL (1995) The controls on the major and trace element evolution of shales, siltstones and sandstones of Ordovician to Tertiary age in the Wet Mountain region, Colorado, U.S.A. Chem Geol 123:107–131

Cullers RL (2000) The geochemistry of shales, siltstones and sandstones of Pennsylvanian-Permian age, Colorado, U.S.A.: implications for provenance and metamorphic studies. Lithos 51:305–327

De Baar HJW, Bacon MP, Brewer PG (1985) Rare earth elements in the Pacific and Atlantic oceans. Geochim Cosmochim Acta 49:1943–1959

De Baar HJW, German CR, Elderfield H, Van Gaans P (1988) Rare earth element distributions in anoxic waters of the Cariaco Trench. Geochim Cosmochim Acta 52:1203–1219

De Baar HJW, Schijf J, Byrne RH (1991) Solution chemistry of the rare earth elements in seawater. Eur J Solid State Inorg Chem 28:357–373

Dubertret L (1966) Liban, Syrie et bordure des pays voisins. Première partie. Tableau stratigraphique avec carte géologique au millionième. Notes et Mém. Moyen-Orient 8: 251–358

Dupré B, Gaillardet J, Rousseau D, Allègre CJ (1996) Major and trace elements of river-borne material: the Congo Basin. Geochim Cosmochim Acta 60:1301–1321

Edgell HS (1977) The Permian system as an oil and gas reservoir in Iran, Iraq and Arabia. Proc. Second Iranian Geological Symposium, Tehran, pp 161–201

Elderfield H (1988) The oceanic chemistry of the rare-earth elements. Phil Trans R Soc London 325:105–126

Elderfield H, Upstill-Goddard R, Sholkovitz ER (1990) The rare-earth elements in rivers, estuaries, and coastal seas and their significance to the composition of ocean waters. Geochim Cosmochim Acta 54: 971–991

Frust M (1970) Stratigraphic und wedegang der ostlichen Zagrosketten (Iran), vol 80. Geologische Abhandlungen Hessen, Erlanger, pp 1–51

Fu X, Wang J, Zeng Y, Tan F, He J (2010) Geochemistry and origin of rare earth elements (REEs) in the Shengli River oil shale, northern Tibet, China. Chem Erde-Geochem 71(1):21–30

German CR, Elderfield H (1989) Rare earth elements in Saanich Inlet, British Columbia, a seasonally anoxic basin. Geochim Cosmochim Acta 53:2561–2571

German CR, Elderfield H (1990) Application of the Ce anomaly as a paleoredox indicator: the ground rules. Paleoceanography 5:823–833

Greaves MJ, Elderfield H, Sholkovitz ER (1999) Aeolian sources of rare earth elements to the Western Pacific Ocean. Mar Chem 68:31–38

Hamza NM, Issac EA (1971) Geological survey of the area between Benavi Village and Greater Zab River. Manuscript report GEOSURV, Baghdad

Holser WT (1997) Evaluation of the application of rare-earth elements to paleoceanography. Palaeogeogr Palaeoclimatol Palaeoecol 132: 309–323

Hua G, Yuansheng D, Lian Z, Jianghai Y, Hu H (2013) Trace and rare earth elemental geochemistry of carbonate succession in the Middle Gaoyuzhuang Formation, Pingquan Section: implications for Early Mesoproterozoic ocean redox conditions. J Palaeogeogr 2:209–221

Jassim SZ, Goff JC (2006) Geology of Iraq. Dolin, Prague and Moravian Museum, Brno, p 341

Jassim SZ, Buday T, Cichea I, Prouza V (2006) Late Permian-Liassic Megasequence AP6. In: Jassim SZ, Goff J (eds) Regional geology of Iraq. Dolin, Prague and Moravian Museum, Brno, pp 104–116

Kamber BS, Webb GE (2001) The geochemistry of late Archaean microbial carbonate: implications for ocean chemistry and continental erosion history. Geochim Cosmochim Acta 65:2509–2525

Kemp RA, Trueman CN (2003) Rare earth elements in Solnhofen biogenic apatite: geochemical clues to the palaeoenvironment. Sediment Geol 155:109–127

Liu YG, Miah MRU, Schmitt RA (1988) Cerium, a chemical tracer for paleo-oceanic redox conditions. Geochim Cosmochim Acta 52: 1361–1371

Madhavaraju J, González-León CM (2012) Depositional conditions and source of rare earth elements in carbonate strata of the Aptian-Albian Mural Formation, Pitaycachi section, northeastern Sonora, Mexico. Revista Mexicana de Ciencias Geológicas 29(2):478–491

Madhavaraju J, Lee YI (2009) Geochemistry of the Dalmiapuram Formation of the Uttatur Group (Early Cretaceous), Cauvery basin, southeastern India: implications on provenance and paleo-redox conditions. Revista Mexicana de Ciencias Geológicas 26:380–394

Madhavaraju J, Ramasamy S (1999) Rare earth elements in limestones of Kallankurichchi Formation of Ariyalur Group, Tiruchirapalli Cretaceous, Tamil Nadu. J Geol Soc India 54:291–301

Madhavaraju J, González-León CM, Lee YI, Armstrong-Altrin JS, Reyes-Campero LM (2010) Geochemistry of the Mural Formation (Aptian-Albian) of the Bisbee Group, Northern Sonora, Mexico. Cretac Res 31:400–414

Masuzawa T, Koyama M (1989) Settling particles with positive Ce anomalies from the Japan Sea. Geophys Res Lett 16:503–506

Mazumdar A, Tanaka K, Takahashi T, Kawabe I (2003) Characteristics of rare earth element abundances in shallow marine continental platform carbonates of Late Neoproterozoic successions from India. Geochem J 37:277–289

McLennan SM (1989) Rare earth elements in sedimentary rocks: influence of provenance and sedimentary processes. Rev Mineral Geochem 21(1):169–200

Morad S, Al-Aasm IS, Sirat M, Sattar MM (2010) Vein calcite in Cretaceous carbonate reservoirs of Abu Dhabi: record of origin of fluids and diagenetic conditions. J Geochem Explor 106:156–170

Murphy K, Dymond J (1984) Rare earth element fluxes and geochemical budget in the eastern equatorial Pacific. Nature 307:444–447

Murray RW, Buchholtz Brink MR, Brink MR, Jones DL, Gerlach DC, Russ GP (1990) Rare earth elements as indicators of different marine depositional environments in chert and shale. Geology 18:268–271

Murray RW, Buchholtz MR, Brumsack HJ (1991) Rare earth elements in Japan Sea sediments and diagenetic behavior of Ce/Ce*, results from ODP leg 127. Geochim Cosmochim Acta 55:2453–2466

Murray RW, Buchholtz Ten Brink MR, Gerlach DC, Russ GP, Jones DL (1992) Interoceanic variation in the rare earth, major and trace element depositional chemistry of chert: perspectives gained from the DSDP and ODP record. Geochim Cosmochim Acta 56:1897–1913

Nagarajan R, Madhavaraju J, Armstron-Altrin JS, Nagendra R (2011) Geochemistry of Neoproterozoic limestones of the Shahabad Formation, Bhima Basin, Karnataka, southern India. Geosci J 15: 9–25

Nath BN, Roelandts I, Sudhakar M, Plueger WL (1992) Rare earth element patterns of the Central Indian Basin sediments related to their lithology. Geophys Res Lett 19:1197–1200

Nath BN, Bau M, Ramalingeswara RB, Rao CM (1997) Trace and rare earth elemental variation in Arabian Sea sediments through a transect across the oxygen minimum zone. Geochim Cosmochim Acta 61:2375–2388

Nothdurft LD, Webb GE, Kamber BS (2004) Rare earth element geochemistry of Late Devonian reefal carbonates, canning basin, Western Australia: confirmation of a seawater REE proxy in ancient limestones. Geochim Cosmochim Acta 68(2):263–283

Palmer MR (1985) Rare earth elements in foraminifera tests. Earth Planet Sci Lett 73:285–298

Powers RW, Ramirez LF, Redmond CD, Elberg EL (1966) Sedimentary geology of Saudi Arabia. In: The geology of the Arabian peninsula. USGS Prof. Paper No.560-D, Washington, p 177

Scherer M, Seitz H (1980) Rare-earth element distribution in Holocene and Pleistocene corals and their distribution during diagenesis. Chem Geol 28:279–289

Schieber J (1988) Redistribution of rare earth elements during diagenesis of carbonate rocks from Mid-Proterozoic Newland Formation, Montana, USA. Chem Geol 69:111–126

Sharland PR, Archer R, Casey DM, Davies RB, Hall SH, Heward AP, Horbury AD, Simmons MD (2001) Arabian plate sequence stratigraphy. GeoArabia, Special Publication 2, Bahrain, p 371

Sholkovitz ER (1988) Rare earth elements in the sediments of the North Atlantic Ocean, Amazon delta, and East China Sea: reinterpretation of terrigenous input patterns to the oceans. Am J Sci 288:236–281

Sholkovitz ER (1990) Rare earth elements in marine sediments and geochemical standards. Chem Geol 88:333–347

Sholkovitz ER, Landing WM, Lewis BL (1994) Ocean particle chemistry: the fractionation of the rare earth elements between suspended particles and seawater. Geochim Cosmochim Acta 58:1567–1580

Taylor SR, McLennan SM (1985) The continental crust: its composition and evolution. Blackwell Scientific Publications, Oxford, p 312

Toyoda K, Nakamura Y, Masuda A (1990) Rare earth elements of Pacific pelagic sediments. Geochim Cosmochim Acta 54:1093–1103

Wanty RB, Goldhaber MB (1992) Thermodynamics and kinetics of reactions involving vanadium in natural systems: accumulation of vanadium in sedimentary rocks. Geochim Cosmochim Acta 56(4): 1471–1483

Webb GE, Kamber BS (2000) Rare earth elements in Holocene reefal microbialites: a new shallow seawater proxy. Geochim Cosmochim Acta 64:1557–1565

Wignall PB, Myers KJ (1988) Interpreting the benthic oxygen levels in mudrocks, a new approach. Geology 16:452–455

Wright J, Seymour RS, Shaw HI (1984) REE and Nd isotopes in cono-
    dont apatite variations with geological age and depositional environ-
    ment. Geol Soc Am Spec Pap 196:325–340
Wronkiewicz DJ, Condie KC (1990) Geochemistry and mineralogy of
    sediments from the Ventersdorp and Transvaal Supergroups, South
    Africa: cratonic evolution during the early Proterozoic. Geochim
    Cosmochim Acta 54:343–354

Zhang J, Nozaki Y (1998) Behavior of rare earth elements in
    seawater at the ocean margin: a study along the slopes of
    the Sagami and Nankai troughs near Japan. Geochim
    Cosmochim Acta 62:1307–1317
Zhao YY, Zheng YF, Chen F (2009) Trace element and strontium isotope
    constraints on sedimentary environment of Ediacaran carbonates in
    southern Anhui, South China. Chem Geol 265:345–362